



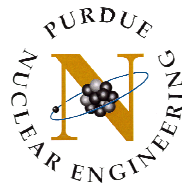
NUCL 511

Nuclear Reactor Theory and Kinetics

Lecture Note 10

Prof. Won Sik Yang

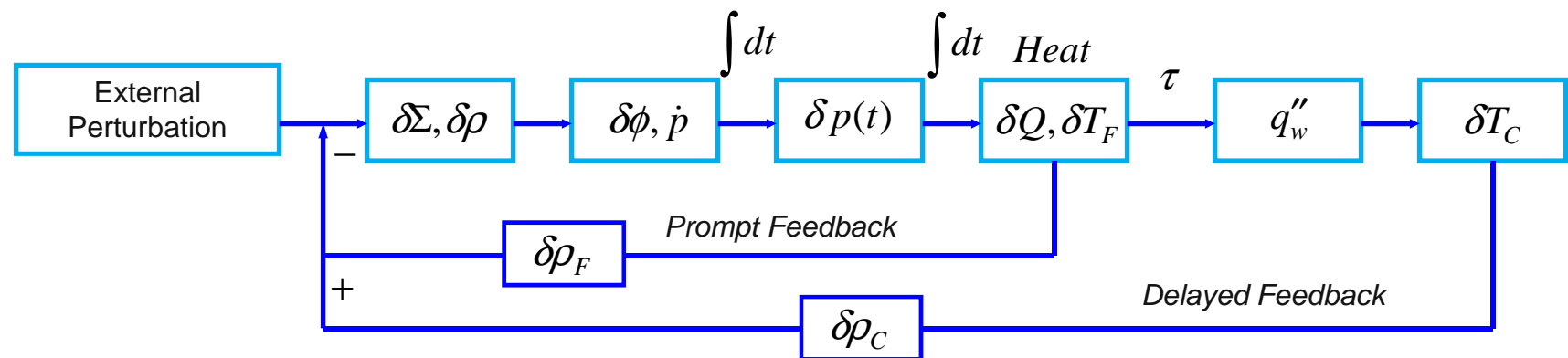
**Purdue University
School of Nuclear Engineering**



PURDUE
UNIVERSITY

Reactivity Feedback Mechanism

- What is reactivity feedback?
 - Reactivity change induces changes in thermal condition which can affect back to the reactivity → thermal feedback
- Feedback Mechanism



- Prompt feedback
 - Occurs immediately due to fuel temperature change
- Delayed feedback
 - Heat conduction to coolant takes time
 - Caused by coolant density change (thermal expansion) which changes moderation or leakage

Doppler Broadening

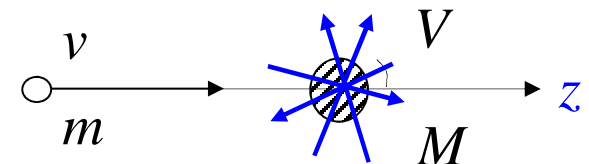
- The laboratory cross section should be defined to agree with the observed reaction rate.
 - The cross section is determined by the relative speed, as opposed to the laboratory speed of neutron
 - The Doppler broadened cross section will not generally be the same as the cold cross section
- If $P(\vec{V})d\vec{V}$ is the probability at temperature T that a nucleus (or atom) has velocity \vec{V} within $d\vec{V}$ about \vec{V} , the observed reaction rate that a neutron with velocity \vec{v} will collide with a nucleus is

$$R(v, T) = v\sigma(v, T) = \int [v_r \sigma(v_r, 0)] P(\vec{V}) d\vec{V}$$

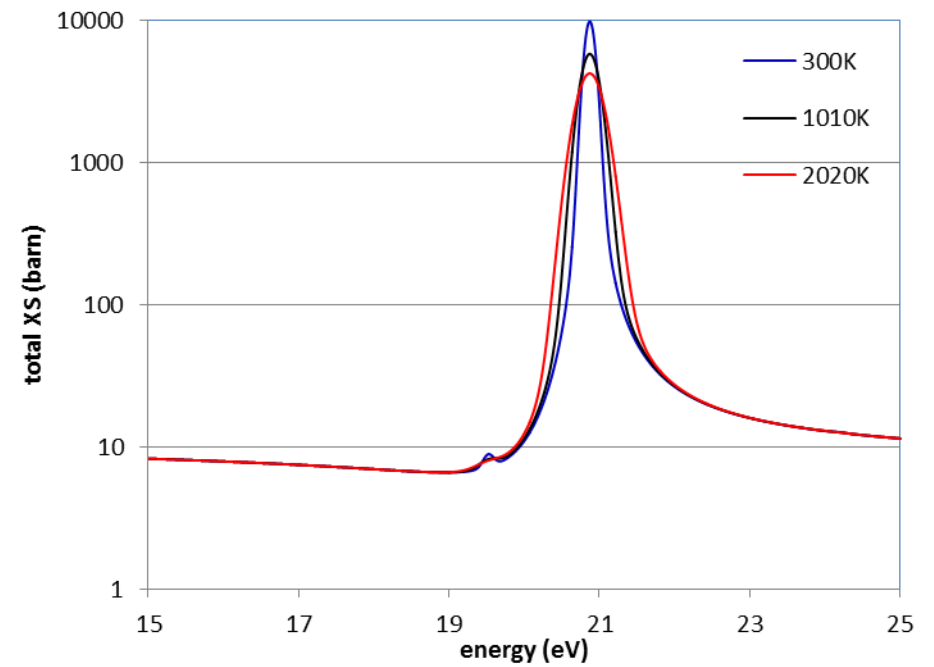
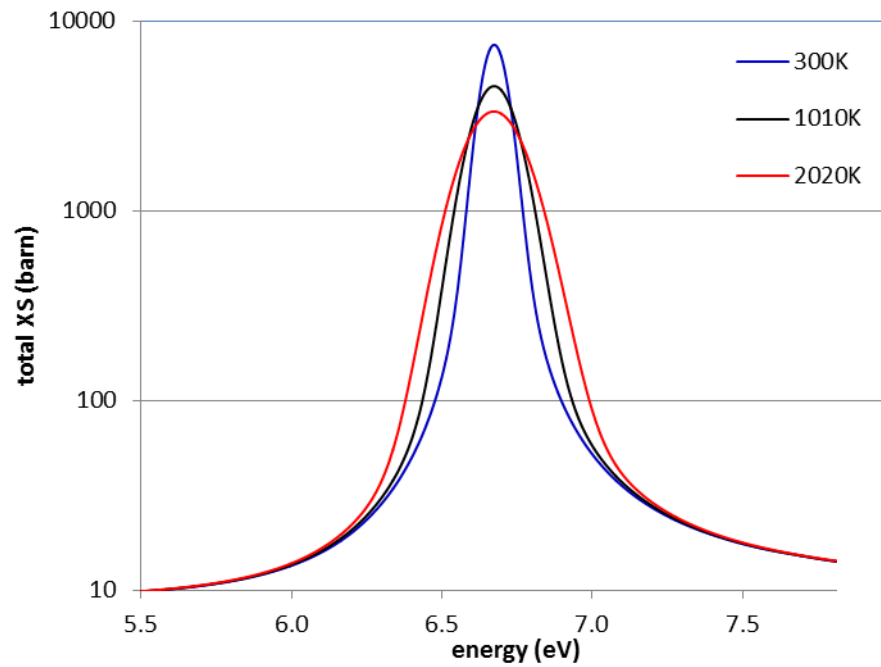
- If the velocity distribution of the target nuclei is isotropic, we have

$$P(\vec{V})d\vec{V} = \frac{1}{4\pi} P(V) dV d\mu d\phi$$

$$\sigma(v, T) = \frac{1}{2v} \int_{-1}^1 d\mu \int_0^\infty dV [v_r \sigma(v_r, 0)] P(V)$$



Doppler Broadened U-238 Total XS



Free Gas Model

- The relative speed can be written as

$$v_r = |\vec{v} - \vec{V}| = (v^2 + V^2 - 2vV\mu)^{1/2}$$

- The Jacobian transformation from the cosine of scattering angle to the relative speed is given by

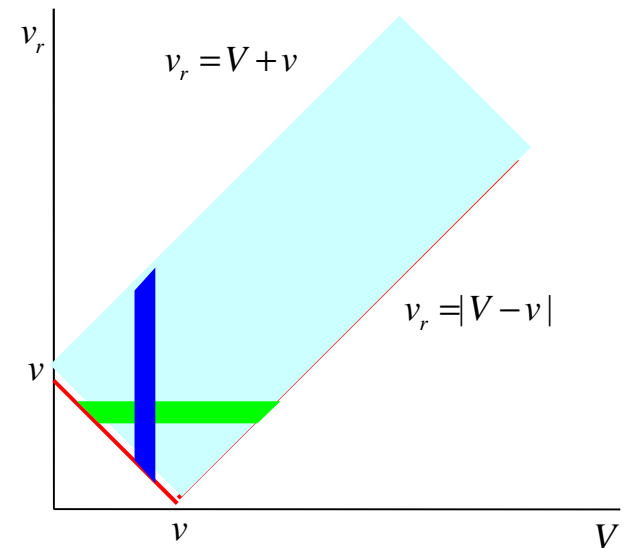
$$d\mu = v_r dv_r / vV$$

- Changing the integration variable from μ to v_r , we have

$$\begin{aligned}\sigma(v, T) &= \frac{1}{2v^2} \int_{|v-V|}^{v+V} [v_r \sigma(v_r, 0)] v_r dv_r \int_0^\infty P(V) \frac{dV}{V} \\ &= \frac{1}{2v^2} \int_0^\infty [v_r \sigma(v_r, 0)] v_r dv_r \int_{|v-v_r|}^{v+v_r} P(V) \frac{dV}{V}\end{aligned}$$

- For the **Maxwellian monatomic (or free) gas model**, the distribution of nuclei speed is given by

$$P(V)dV = 4\pi \left(\frac{a}{\pi} \right)^{3/2} V^2 e^{-aV^2} dV; \quad a = \frac{M}{2kT}$$



Doppler Broadened Cross Section

- The Doppler broadened cross section is obtained as

$$\begin{aligned}\sigma(v, T) &= \frac{2a^{3/2}}{\sqrt{\pi}v^2} \int_0^\infty [v_r \sigma(v_r, 0)] v_r dv_r \int_{|v-v_r|}^{v+v_r} V e^{-aV^2} dV \\ &= \frac{a^{1/2}}{\sqrt{\pi}v^2} \int_0^\infty [v_r \sigma(v_r, 0)] v_r \left[e^{-a(v-v_r)^2} - e^{-a(v+v_r)^2} \right] dv_r\end{aligned}$$

- This can be rewritten in terms of energy as

$$\sigma(E, T) = \frac{\alpha^{1/2}}{2\sqrt{\pi}E} \int_0^\infty [\sqrt{E_r} \sigma(E_r, 0)] \left[e^{-\alpha(\sqrt{E}-\sqrt{E_r})^2} - e^{-\alpha(\sqrt{E}+\sqrt{E_r})^2} \right] dE_r$$

$$E = \frac{1}{2}mv^2; \quad E_r = \frac{1}{2}mv_r^2; \quad \alpha = \frac{2a}{m} = \frac{M}{mkT} = \frac{A}{kT}$$

- For large $\alpha\sqrt{EE_r}$ ($\sim AE / kT$), the second exponential can be ignored, compared to the first

$$\sigma(E, T) = \frac{\alpha^{1/2}}{2\sqrt{\pi}E} \int_0^\infty [\sqrt{E_r} \sigma(E_r, 0)] e^{-\alpha(\sqrt{E}-\sqrt{E_r})^2} dE_r$$

Single Level Breit-Wigner Formula

■ Doppler broadened cross section

$$\sigma(E, T) = \frac{1}{\Delta \sqrt{\pi E}} \int_{-\infty}^{\infty} [\sqrt{E_r} \sigma(E_r)] e^{-[(E_r - E)/\Delta]^2} dE_r$$

$$\Delta = \left(\frac{4kTE}{A} \right)^{1/2} \quad (\text{Doppler width})$$

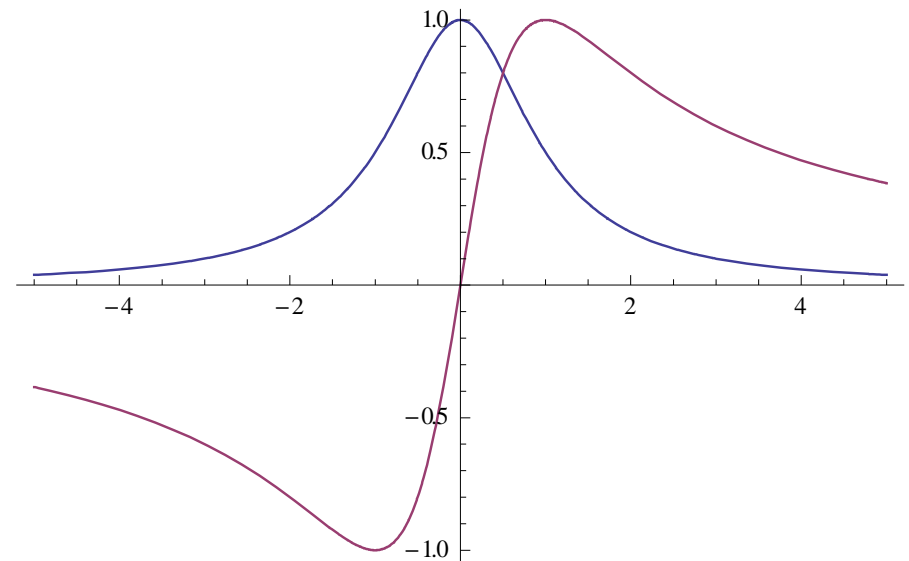
■ Single level Breit-Wigner formula

$$\sigma_a(E_r) \approx \sigma_0 \frac{\Gamma_a}{\Gamma} \frac{1}{1 + w^2} \quad (a = \gamma, f)$$

$$\sigma_n(E_r) \approx 4\pi a^2 + \sigma_0 \frac{\Gamma_n}{\Gamma} \frac{1}{1 + w^2} + \sigma_0 k a \frac{2w}{1 + w^2}$$

$$w = \frac{E_r - E_0}{\Gamma / 2}$$

$$\sigma_0 = \frac{4\pi}{k^2} g_J \frac{\Gamma_n}{\Gamma} \quad (\text{resonance peak}), \quad k = \frac{2\pi}{\lambda} \quad (\text{wave number})$$



Doppler Broadened Line Shape Functions

■ Doppler broadened cross sections

$$\sigma_a(E, T) = \sigma_0 \frac{\Gamma_a}{\Gamma} \sqrt{\frac{E_0}{E}} \psi(x, \xi), \quad (a = \gamma, f)$$

$$\sigma_n(E, T) = 4\pi a^2 + \sigma_0 \frac{\Gamma_n}{\Gamma} \psi(x, \xi) + 2\sigma_0 k a \chi(x, \xi)$$

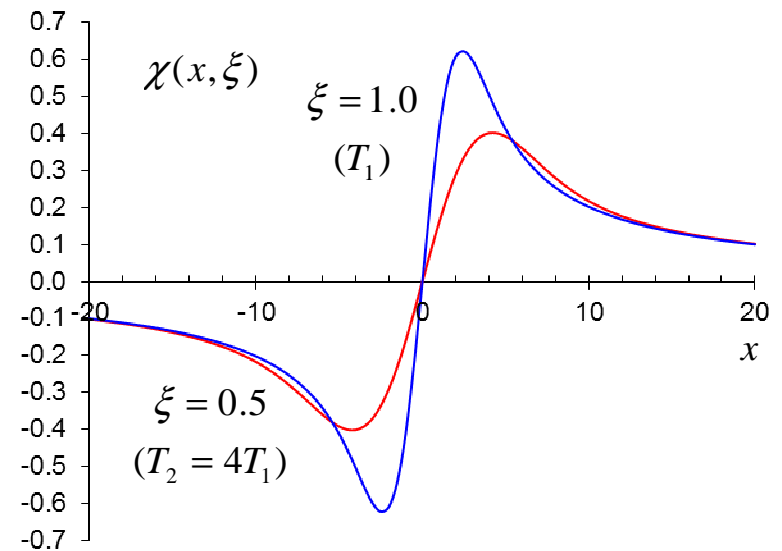
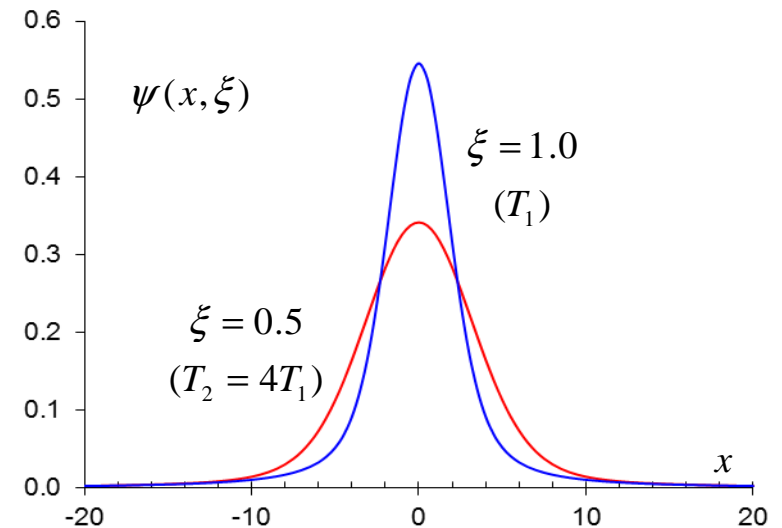
$$x = \frac{E - E_0}{\Gamma/2}, \quad \xi = \frac{\Gamma}{\Delta}, \quad \sqrt{\frac{E_0}{E}} \approx 1$$

■ Symmetric and anti-symmetric Doppler broadened line shape functions

$$\psi(x, \xi) = \frac{\xi}{2\sqrt{\pi}} \int_{-\infty}^{\infty} \frac{1}{1+w^2} \exp\left[-\frac{\xi^2}{4}(x-w)^2\right] dw$$

$$\chi(x, \xi) = \frac{\xi}{\sqrt{\pi}} \int_{-\infty}^{\infty} \frac{w}{1+w^2} \exp\left[-\frac{\xi^2}{4}(x-w)^2\right] dw$$

$$\sqrt{E_r} \approx \sqrt{E_0}$$



Psi-Chi Functions

- Doppler broadened line shape functions can be represented as convolution integrals of Lorentzian L and Gaussian kernel G as

$$\psi(x, \xi) = \int_{-\infty}^{\infty} L(w)G(x-w; \xi)dw = L(x) * G(x, \xi)$$

$$\chi(x, \xi) = \int_{-\infty}^{\infty} 2wL(w)G(x-w, \xi)dw = [2xL(x)] * G(x, \xi)$$

$$L(x) = \frac{1}{1+x^2} \text{ (natural line shape), } G(x, \xi) = \frac{\xi}{2\sqrt{\pi}} \exp\left(-\frac{\xi^2}{4}x^2\right) \text{ (pure Doppler shape)}$$

- At a very low temperature ($\xi = \Gamma_t / \Delta \gg 1$), the Doppler broadened line shapes reduce to the natural line shapes

$$\lim_{\xi \rightarrow \infty} \psi(x, \xi) = \int_{-\infty}^{\infty} L(w)\delta(x-w)dw = L(x), \quad \lim_{\xi \rightarrow \infty} \chi(x, \xi) = \int_{-\infty}^{\infty} 2wL(w)\delta(x-w)dw = 2xL(x)$$

- At a very high temperature ($\xi = \Gamma_t / \Delta \ll 1$), the Doppler broadened line shapes reduce to the pure Doppler shapes

$$\lim_{\xi \rightarrow 0} \psi(x, \xi) = \frac{\xi\sqrt{\pi}}{2} \int_{-\infty}^{\infty} \delta(t) \exp\left[-\frac{1}{4}(\xi x - t)^2\right] dt = \pi G(x, \xi)$$

$$\lim_{\xi \rightarrow 0} \chi(x, \xi) = \sqrt{\pi} \int_{-\infty}^{\infty} \delta(t) t \exp\left[-\frac{1}{4}(\xi x - t)^2\right] dt = 0$$

Self-Shielding Factor

- Group-averaged cross section is computed

$$\sigma_{xg}^i(T, \sigma_b) = \frac{\int_g \sigma_x^i(E, T) \phi_i(E, T, \sigma_b) dE}{\int_g \phi_i(E, T, \sigma_b) dE} = \frac{\int_g \sigma_x^i(E, T) C(E) / [\sigma_b + \sigma_t^i(E, T)] dE}{\int_g C(E) / [\sigma_b + \sigma_t^i(E, T)] dE}$$

- Traditional J-integral approach for SLBW resonances

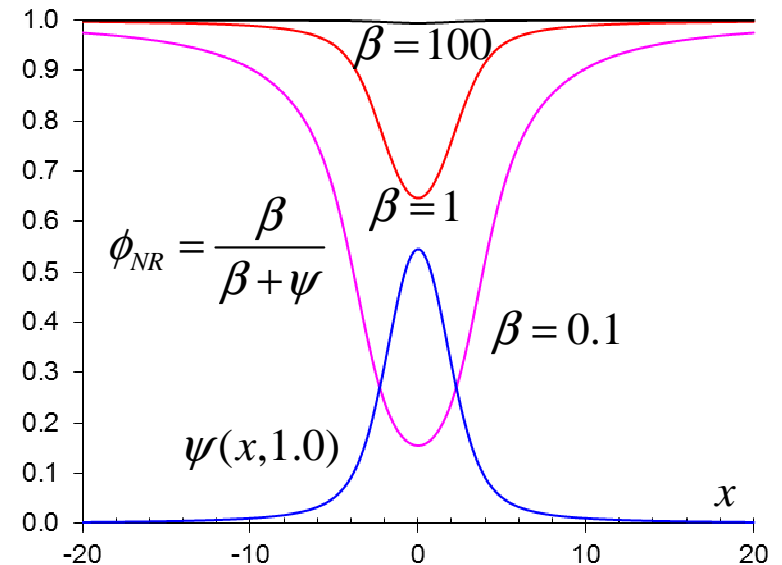
$$I_k^i(T, \sigma_b) = C \int \frac{\sigma_t^i(E, T)}{\sigma_b + \sigma_t^i(E, T)} dE = C \frac{\Gamma}{2} \int \frac{\sigma_0^i \psi(x, \xi)}{\sigma_b + \sigma_0^i \psi(x, \xi)} dx = C \Gamma J(\beta, \xi)$$

$$J(\xi, \beta) = \int_0^\infty \frac{\psi(x, \xi)}{\beta + \psi(x, \xi)} dx, \quad \beta = \frac{\sigma_b}{\sigma_0^i}$$

$$\lim_{\beta \rightarrow \infty} J(\xi, \beta) = \frac{1}{2\beta} \int_{-\infty}^\infty \psi(x, \xi) dx = \frac{\pi}{2\beta}$$

- Self-shielding factor

$$f(T, \sigma_b) = \frac{\sigma(T, \sigma_b)}{\sigma(0, \infty)} \approx \frac{2\beta}{\pi} J(\xi, \beta)$$

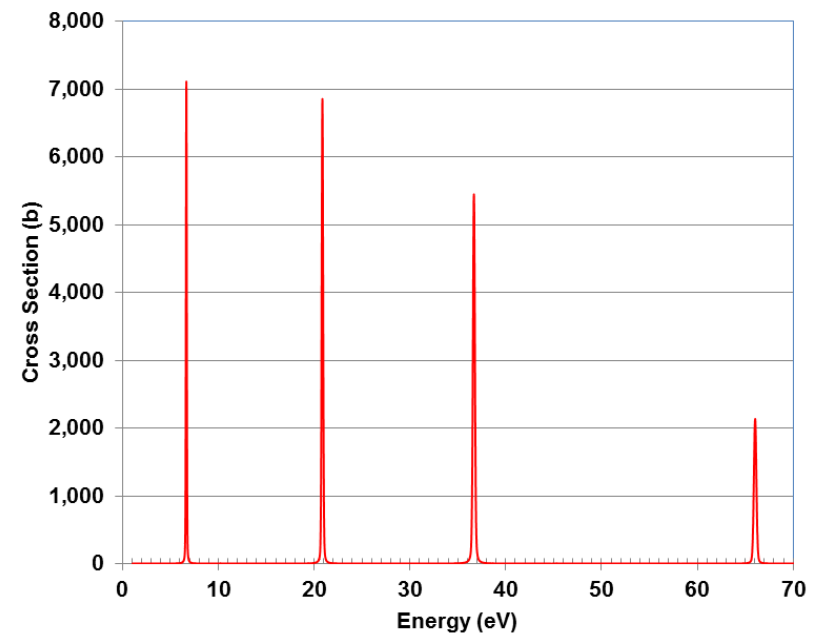
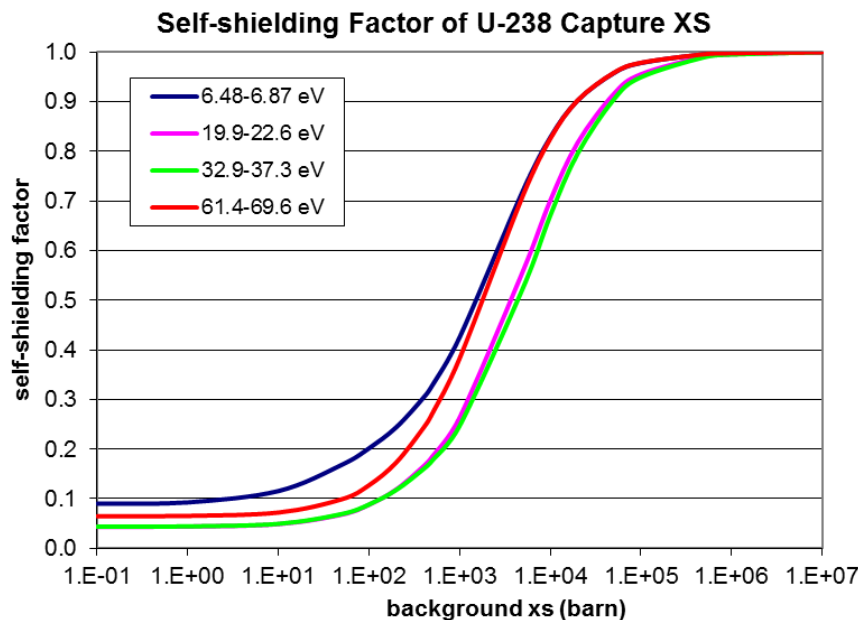


Background Cross Section Dependence

- Absorption decreases with increasing background cross section
 - Self-shielding factor increases

$$\frac{\partial J}{\partial \beta} = - \int_0^{\infty} \frac{\psi(x, \xi)}{[\beta + \psi(x, \xi)]^2} dx < 0$$

$$\frac{\partial f}{\partial \beta} = \frac{\partial}{\partial \beta} \left[\frac{2\beta}{\pi} J \right] = \frac{2}{\pi} \left[J + \beta \frac{\partial J}{\partial \beta} \right] = \int_0^{\infty} \left[\frac{\psi(x, \xi)}{\beta + \psi(x, \xi)} \right]^2 dx > 0$$



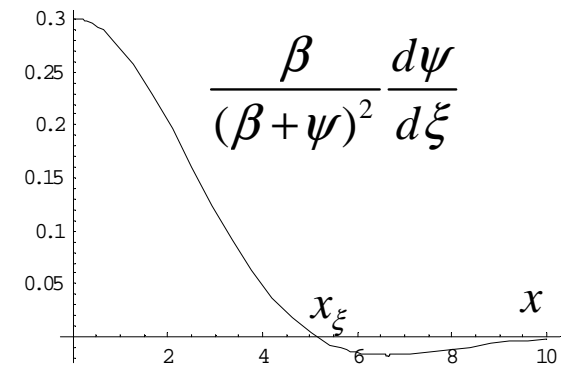
Temperature Dependence

- Absorption increases with increasing temperature
 - Reactivity decreases and thus the Doppler coefficient is negative

$$\frac{\partial J}{\partial \xi} = \int_0^{\infty} \frac{\beta}{[\beta + \psi(x, \xi)]^2} \frac{\partial \psi}{\partial \xi} dx = \int_0^{x_\xi} f(x) \frac{\partial \psi}{\partial \xi} dx - \int_{x_\xi}^{\infty} f(x) \left| \frac{\partial \psi}{\partial \xi} \right| dx$$

$$< f(x_\xi) \int_0^{x_\xi} \frac{\partial \psi}{\partial \xi} dx - f(x_\xi) \int_{x_\xi}^{\infty} \left| \frac{\partial \psi}{\partial \xi} \right| dx = f(x_\xi) \int_0^{\infty} \frac{\partial \psi}{\partial \xi} dx = 0$$

$$\frac{\partial}{\partial T} J(\xi, \beta) = \frac{\partial J}{\partial \xi} \frac{d\xi}{dT} = -\frac{\Gamma_t}{2} \left(\frac{A}{4kE} \right)^{1/2} T^{-3/2} \frac{\partial J}{\partial \xi} > 0$$



- Self-shielding effect decreases with increasing temperature
 - Self-shielding factor increases

$$\frac{\partial f}{\partial T} = \frac{\partial}{\partial \xi} \left[\frac{2\beta}{\pi} J \right] \frac{d\xi}{dT} = -\frac{\beta \Gamma_t}{\pi} \left(\frac{A}{4kE} \right)^{1/2} T^{-3/2} \frac{\partial J}{\partial \xi} > 0$$

Low Temperature

- At a very low temperature, $\xi \gg 1$ and the Doppler broadened line shape reduces to the natural line shape.
- In this case, the J function and self-shielding factor become

$$\lim_{\xi \rightarrow \infty} J(\xi, \beta) = \int_0^\infty \frac{L(x)}{\beta + L(x)} dx = \frac{1}{\beta} \int_0^\infty \frac{dx}{(1 + \beta^{-1}) + x^2} = \frac{\pi}{2\beta(1 + \beta^{-1})^{1/2}}$$

$$f(\infty, \beta) = \left(\frac{\beta}{1 + \beta} \right)^{1/2} \approx \begin{cases} \sqrt{\beta} & \text{for small } \beta \\ 1 - \frac{1}{2\beta} & \text{for large } \beta \end{cases}$$

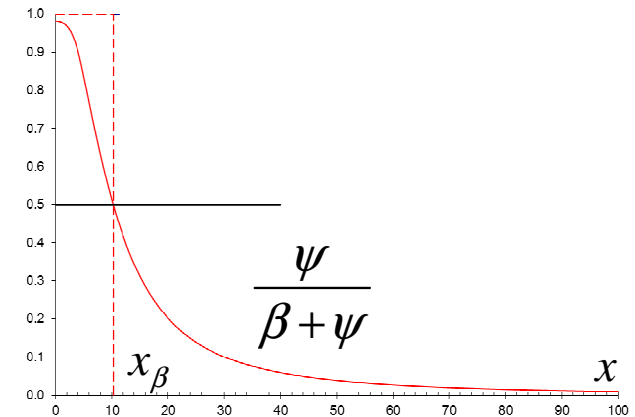
- This eliminates the temperature dependence from the self-shielding factor.
 - The resonance is un-broadened and has its maximum height.
 - This leads to the strongest self-shielding and thus to the smallest value of the self-shielding factor

High Resonances at Low Energies

- For high resonances ($\beta \ll 1$) at low energies, the integrand of the J function is close to 1 for the high part of the resonance. The integrand decreases on the resonance wings, becomes equal to 1/2 where $\psi(x_\beta, \xi) = \beta$, and vanishes asymptotically.

- The J integral can be approximated by the area of the rectangle of height 1 and width x_β
- x_β can be determined from the approximation for dominating Doppler broadening

$$\beta = \psi(x_\beta, \xi) \approx \frac{\sqrt{\pi}\xi}{2} \exp\left(-\frac{\xi^2}{4} x_\beta^2\right)$$



$$J(\xi, \beta) \approx x_\beta \approx \frac{2}{\xi} \sqrt{\ln \frac{\sqrt{\pi}\xi}{2\beta}} \propto \frac{1}{\xi} \propto \sqrt{T}, \quad \frac{\partial}{\partial T} J(\xi, \beta) \propto \frac{1}{\sqrt{T}}$$

- Since high resonances dominate in the $1/E$ spectrum of thermal reactors, the resonance integral in thermal reactors depends on temperature through a \sqrt{T} term, and the Doppler coefficient has a temperature dependence as $1/\sqrt{T}$

Low Resonances at High Energies

- For resonances which are much lower than the potential cross section, $\beta \gg \psi$ and hence the J function can be approximated as

$$J(\xi, \beta) = \int_0^\infty \frac{\psi}{\beta + \psi} dx = \frac{1}{\beta} \int_0^\infty \frac{\psi}{1 + (\psi / \beta)} dx \approx \frac{1}{\beta} \int_0^\infty \psi \left(1 - \frac{\psi}{\beta} \right) dx = \frac{\pi}{2\beta} - \frac{\pi}{4\beta^2} \psi(0, \sqrt{2}\xi)$$

- For low resonances at high energies, Doppler broadening generally dominates ($\xi \gg 1$) and hence

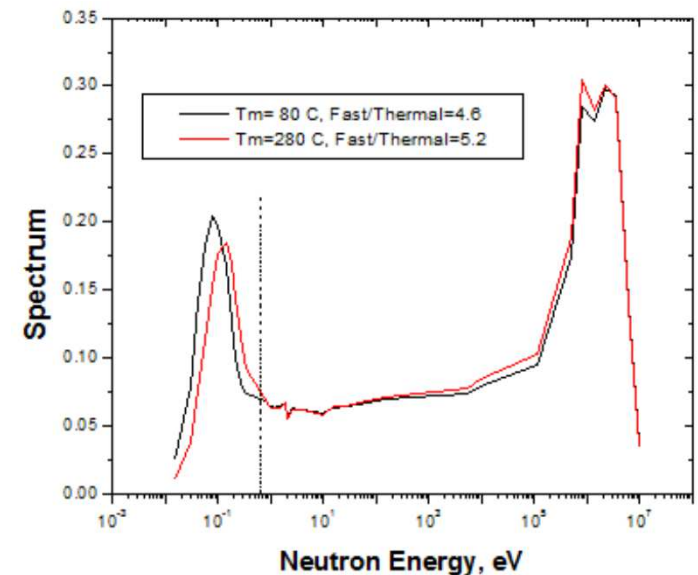
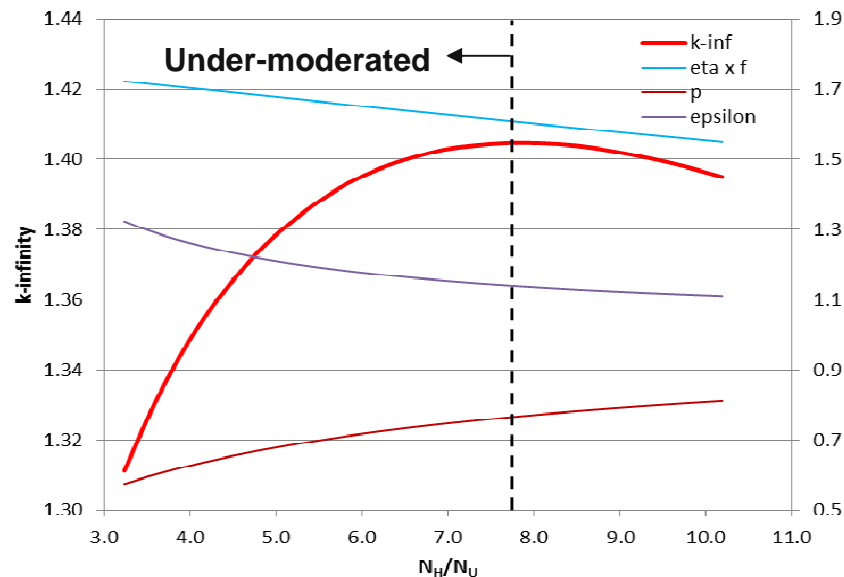
$$\psi(x, \xi) \approx \pi G(x, \xi) = \frac{\xi \sqrt{\pi}}{2} \exp\left(-\frac{1}{4} \xi^2 x^2\right) \Rightarrow \psi(0, \sqrt{2}\xi) \approx \sqrt{\frac{\pi}{2}} \xi = \frac{\sqrt{\pi} \Gamma_t}{\sqrt{2}} \left(\frac{A}{4kE}\right)^{1/2} \frac{1}{\sqrt{T}}$$

$$\frac{\partial}{\partial T} J(\xi, \beta) \approx \left(\frac{\pi}{2}\right)^{3/2} \frac{\Gamma_t}{4} \left(\frac{A_i}{4kE}\right)^{1/2} \left(\frac{N_i \sigma_m^k}{\Sigma_p}\right)^2 T^{-3/2}$$

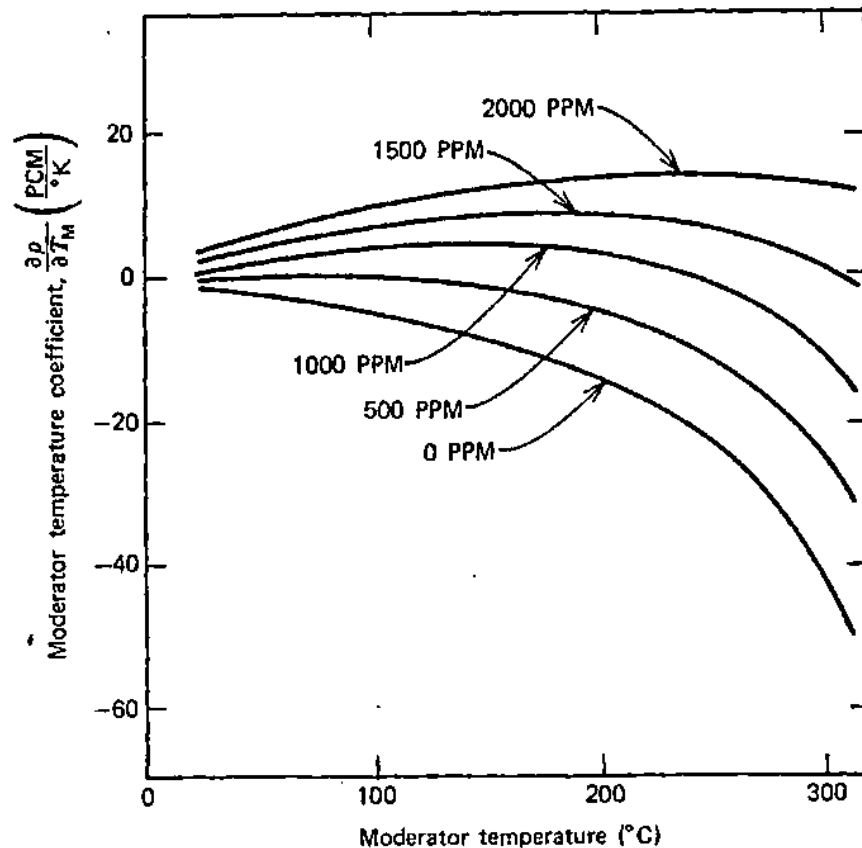
- In the very hard spectrum of small fast reactors, the temperature dependence is determined by the $T^{-3/2}$ contributions of the high energy resonances.
- In the relatively soft neutron spectra of large ceramic fueled fast reactors, it is between the two limiting cases of high resonances ($T^{-3/2}$) and low resonances ($T^{-1/2}$).
- A simple analytical evaluation of the medium height resonances is not feasible. A numerical evaluation of the high, medium, and low resonance contributions to the Doppler coefficient in large fast reactors yields an approximate proportionality to T^{-1}

Moderator Effects

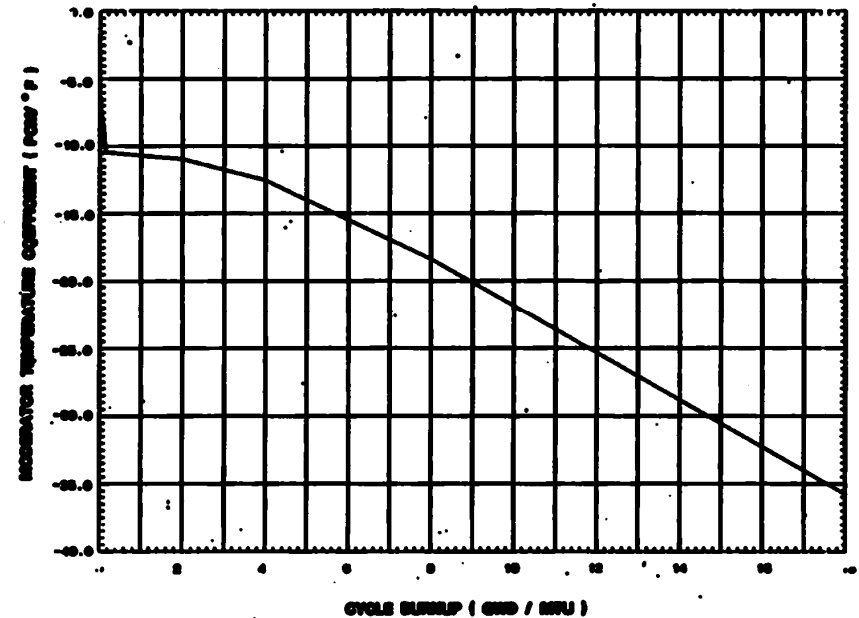
- Change in moderator temperature induces changes in moderator density and scattering kernel
- Fuel-to-moderator ratio in under-moderated region for negative MTC
 - $T_m \uparrow \Rightarrow d_m \downarrow \Rightarrow$ spectrum hardening \Rightarrow resonance absorption $\uparrow \Rightarrow \rho \downarrow$
 - In PWR, $d_m \downarrow \Rightarrow$ boron concentration $\downarrow \Rightarrow \rho \uparrow$
 - MTC becomes less negative as boron concentration increases
 - Boron concentration is limited since MTC can be positive at very high concentration (2500 ppm)



Moderator Temperature Coefficient of PWR

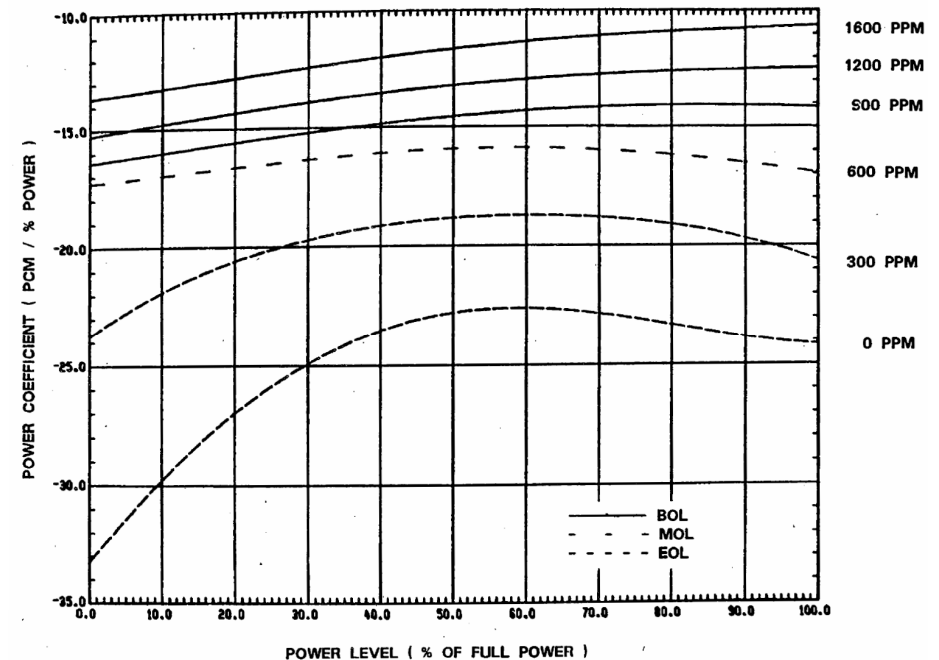
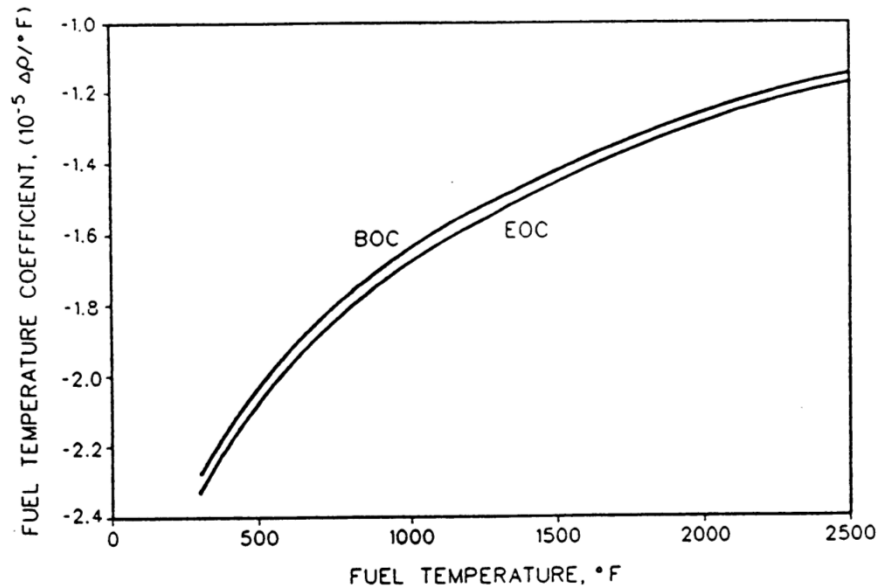


- MTC becomes more positive with boron concentration because of larger reduction in poison content from reduced density (increased temperature)



- MTC becomes more negative with burnup primarily because of the reduction in boron concentration with burnup
- Large negative value would be limiting for a cold water injection incidence
- MTC becomes more negative with control rod insertion because of hardened neutron spectrum and increased leakage

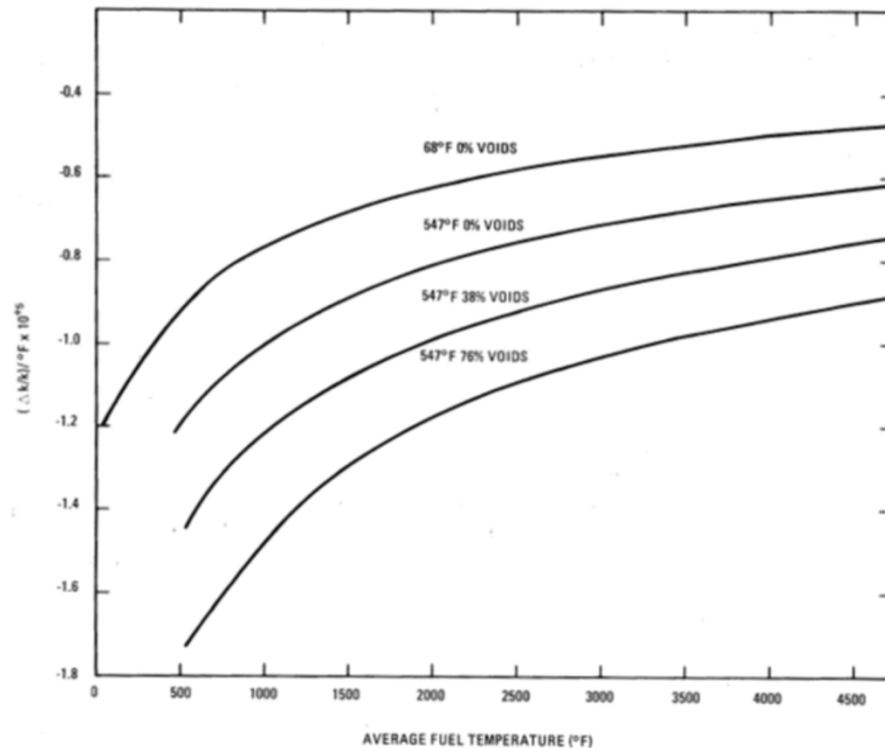
Fuel Temperature and Power Coefficients of PWR



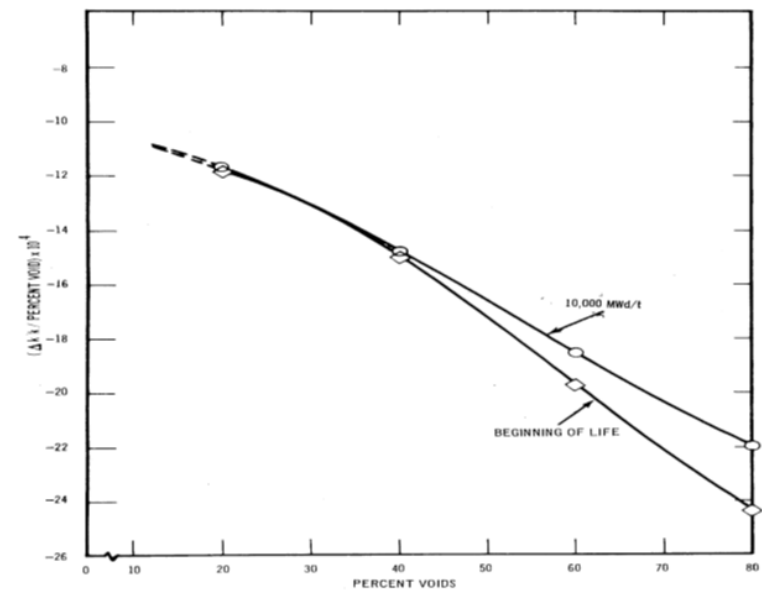
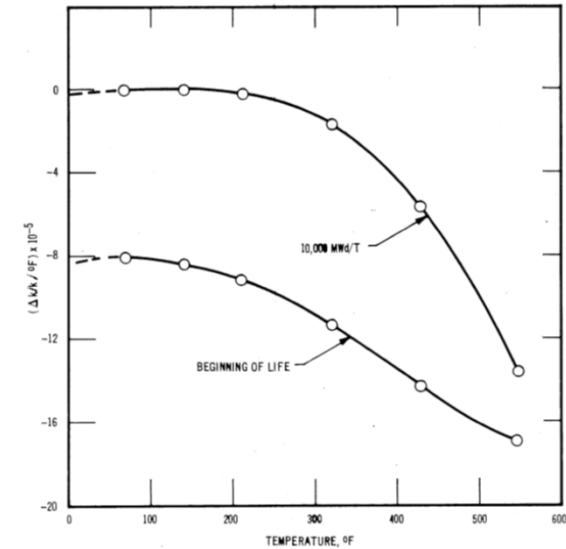
- Magnitude of fuel temperature coefficient decreases with increasing fuel temperature
- Becomes more negative with burnup because of Pu-240 contribution

- Power reactivity coefficient must be negative under all operating conditions
- Coefficient becomes more negative with burnup because of the MTC contribution

Reactivity Feedback Coefficients of BWR



- Coolant temperature coefficient is valid in the core heat-up range
- Void coefficient is valid in the power range of operation



Reactivity Feedback Coefficients of SFR

- The reactivity coefficients and kinetic parameters further define the physics of system
 - Response to a variety of perturbations
- Feedback coefficients are computed for a specific design (geometric and material) configuration
 - Typically evaluated for BOEC and EOEC compositions
- Typical set of whole-core reactivity coefficients
 - Delayed neutron fraction and prompt neutron lifetime
 - Coolant density coefficient and void worth
 - Fuel and structural Doppler coefficient
 - Fuel and structural worth distributions
 - Axial expansion
 - Radial expansion
 - Control rod driveline expansion
- Hummel and Okrent – *Reactivity Coefficients in Large Fast Power Reactors*, ANS, 1970 is a good reference for underlying physics

Neutron Balances of Radial and Axial Expansions

	Base Case	Radial Expansion		Axial Expansion	
	balance	balance	$\Delta\rho$ (%)	balance	$\Delta\rho$ (%)
Fission source	100.00	100.00		100.00	
(n,2n) source	0.18	0.18		0.18	
Absorption	68.89	68.93	-0.04	69.06	-0.17
Leakage	31.54	32.16	-0.63	31.69	-0.16
Radial	17.49	17.72	-0.23	17.65	-0.15
Axial	14.05	14.45	-0.40	14.04	0.01
Sum			-0.67		-0.33

- To first order, radial expansion is an axial leakage effect, and axial expansion is a radial leakage effect
- Because the height is the shorter dimension (more axial than radial leakage), the radial expansion coefficient is more negative
- Axial expansion also give absorption effect from control rod insertion

Coolant Density and Void Coefficients

- Spectral effect
 - Reduced moderation as sodium density decreases
 - In fast regime, this is a positive reactivity effect
 - *From Pu-239 excess neutrons and threshold fission effects*
- Leakage effect
 - Sodium density reduction allows more neutron leakage
 - This is a negative reactivity effect in the peripheral regions
- Capture effect
 - Sodium density decrease results in less sodium capture
 - This is a relatively minor effect
- Coolant density coefficient is computed by first-order perturbation theory to evaluate small density (temperature variation) impacts
- Void worth is evaluated using exact perturbation theory to account for shift in flux distribution for voided condition
 - In general, 10% more positive than the first-order density worth

Sodium Void Worth by Components (\$)

		Capture	Spectral	Leakage	Total
1000 MWt ABR (startup metal core)	BOC	0.5	9.1	-5.2	4.4
	EOC	0.5	9.9	-5.5	4.9
250 MWt ABTR (startup metal core)	BOC	0.4	6.4	-5.8	1.0
	EOC	0.4	6.6	-5.8	1.1

- Flowing sodium was voided in active and above-core regions
- Void worth tends to increase with core size
- However, difficult to conceive transient situations that reach boiling
 - Low pressure system
 - More than 300°C margin to boiling
 - Other feedbacks are negative, inhibiting this temperature increase
- Extensive report on void worth reduction – Khalil and Hill, NS&E, 109 (1995)